ACS OMEGA

http://pubs.acs.org/journal/acsodf

Article

Geological Controls on the Gas Content and Permeability of Coal Reservoirs in the Daning Block, Southern Qinshui Basin

Zhiqi Guo, Yunxing Cao, Zheng Zhang,* and Shi Dong

Cite This: *ACS Omega* 2022, 7, 17063−17074

Read Online

ACCESS | Metrics & More | Article Recommendations

ABSTRACT: The gas content and permeability of the coal reservoir are the key factors affecting coalbed methane (CBM) productivity. To investigate the geological controls on the permeability and gas content of coal reservoirs in the Daning block, southern Qinshui Basin, geological surveys combined with laboratory experiments, including coal petrology analysis, proximate analysis, and methane isothermal adsorption experiments, were carried out. The results show that the gas content of coals in the Daning block ranges from 5.56 to 17.57 (avg. 12.83) m^3/t, and the coal permeability is generally above 0.1 mD, averaging 0.96 mD. The gas content of coal reservoirs shows decreasing trends with the increase in ash yield and moisture content, while tends to increase with the increase of vitrinite content; however, the correlation coefficients are all extremely low. The gas content presents a strong positive correlation with the burial depth of coal seams, but overall poorly correlates with the coal thickness. The CBM-rich areas are generally located at the hinge zones of secondary synclines, while the lower gas content areas commonly occur at the hinge zones of secondary anticlines. The normal faults are developed in the Daning block, and as expected, the gas content of coal seams that are near the normal faults is commonly lower. It was found that the well testing permeability of coal reservoirs in the Daning block decreases exponentially with the increase of the minimum horizontal stress (σ_h) and the maximum horizontal principal stress (σ_H). With the increase of the burial depth, the coal permeability also decreases exponentially. The primary and cataclastic structure coals generally have a higher hydro-fracturing permeability than the granulitic and mylonitic structure coals. This work can serve as a guide for the target area selections of CBM enrichment and high production in the Daning block.

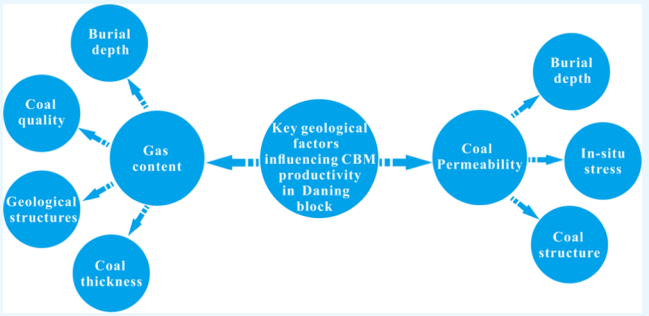

1. INTRODUCTION

The global resources of coalbed methane (CBM) are very rich and amount to 263.8 trillion m^3.[1,2] As a clean energy and a significant supplement to conventional natural gas, the CBM has received extensive attention in many countries worldwide.[3−6] The United States, Canada, and Australia are currently the most successful countries in terms of CBM development in the world.[7] The CBM in China is very abundant, with resources up to 30.05 trillion m^3, ranking the third in the world.[8] To improve the coal-based energy structure, to prevent gas explosion accidents in coal mines, and to reduce the greenhouse effect caused by coal mine methane emissions, China has been increasing the technological and financial investments in CBM exploration and development in the past twenty years.[9−11] The CBM production from surface wells of China is 5.77 billion m^3 in 2020, only accounting for 3.07% of the total natural gas output,[7] and this development scale is not satisfactory at present.[7,12,13]

The rapid growth of CBM production in the United States, Canada, and Australia and their success in high production are due to the discovery of high-abundance CBM enrichment areas in some basins.[14] The CBM enrichment and high production constitute the keys to high-abundance CBM enrichment areas.[14] CBM enrichment depends on the gas content, and the high production of the enriched CBM is mainly controlled by coal permeability.[15] Thus, the gas content and permeability of the coal seams are considered to be the most critical geological controls for CBM productivity.[16] The gas content in the coalbed is influenced by multiple geological factors and reservoir conditions, such as burial depth, coal rank, coal thickness, coal quality, sealing conditions, hydrogeology, structural conditions, etc.[17−22] The factors affecting the permeability of a coal reservoir are more complex. Geological structures, stress state, burial depth of coal seams, coal structure, coal quality, coal rank, and fractures of coal

Received: January 18, 2022
Accepted: April 28, 2022
Published: May 10, 2022

https://doi.org/10.1021/acsomega.2c00371
ACS Omega 2022, 7, 17063−17074

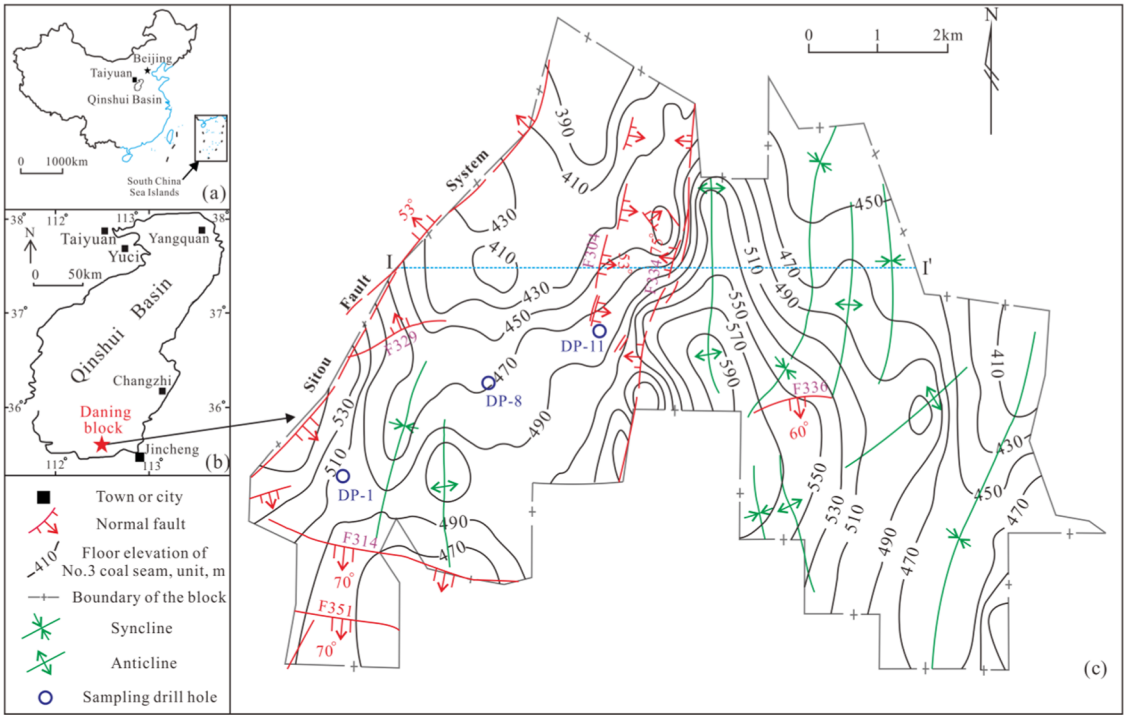

Figure 1. (a) Location of the Qinshui Basin in North China; (b) Location of the Daning block in the southern Qinshui Basin, and (c) The No. 3 coal seam floor contour map with the major structures marked in the Daning block. (modified from ref 1, Copyright (2021), with permission from ACS Omega).

would affect the permeability of coal seams to varying degrees.[23−27] The permeability is the result of a combination of multiple factors, and is sometimes dominated by a certain factor.[23−28]

The CBM resources of Qinshui Basin in North China (Figure 1a) are very huge, reaching 3.28×10^{12} m^3,[26] and they account for approximately 10% of the total CBM resources of China. By 2020, as many as 10 400 surface CBM wells had been drilled in Qinshui Basin and it accounts for more than 60% of the total surface CBM wells in China;[29] meanwhile, CBM production from Qinshui Basin constitutes 80% of the total CBM production of China,[30] making it the most active and successful CBM development basin in China. The optimal location for CBM development in Qinshui Basin is at the southern margin, i.e., southern Qinshui Basin (SQB).[31] Thus, a lot of studies on the CBM geology, resource occurrence conditions, development technologies, etc., have been conducted in different blocks of the SQB.[5,14−16,21,26,27,30,31]

The objective of this work is to analyze the major geological factors affecting the gas content and permeability of the coal reservoir in the Daning block, a relatively new CBM target area in the SQB. The majority of data were obtained from CBM exploration and development wells in the Daning block. In addition, some coals were sampled from the Daning block to conduct laboratory experiments, including proximate analysis, coal petrology analysis, and methane adsorption isotherm experiments. The distribution of gas in the No. 3 coal seam was discussed. The effect of geological controlling factors on the gas content and permeability of coal seams in this area was discussed. This work could serve as a guide for the target area selection of CBM enrichment and high production in the Daning block.

2. GEOLOGICAL SETTINGS

The Qinshui Basin covers an area of approximately 27 000 km^2 and is formed during the period from the middle Jurassic to early Cretaceous,[32] and it is a large synclinorium with an axis strike of NNE-SSW.[5] The Daning block covers an area of approximately 39 km^2 and is situated in the SQB (Figure 1b), tectonically surrounded by the Zhongtiao mountain uplift in the west and Taihang mountain uplift in the east.[26] Overall, the dip direction of the stratum in the study area is north, with a dip angle generally lower than 10°. Structures in the Daning block are relatively simple. Several secondary folds with an axis strike of NE or nearly NS develop in the eastern part; a series of normal faults with a strike of NNE or NE or nearly WE occurs in the western and central parts. The Sitou fault system is the largest fault in the study area and forms the western boundary of the Daning block (Figure 1c).

From bottom to top, the strata in the Daning block include Ordovician Fengfeng (O_{2f}), Carboniferous Benxi (C_{2b}), Carboniferous−Permian Taiyuan (C_2-P_{1t}), Permian Shanxi (P_{1s}), Permian Xiashihezi (P_{1x}), Permian Shangshihexi (P_{2s}), and Permian Shiqianfeng (P_{2sh}) formations, as well as Quaternary. The $C_2 \sim P_{1t}$, P_{1s}, and P_{1x} formations are the major coal-bearing strata, and the No. 3 coal seam in the P_{1s} and the No. 15 coal seam in the C_2-P_{1t} are the main coal reservoirs (Figure 2a). At present, the No. 3 coal seam is the main target layer for CBM exploration and development in the study area.

The coals in the Daning block are typical anthracite, with a maximum vitrinite reflectance ($R_{o,max}$) varying from 2.95 to 3.36%, averaging 3.17%. The organic macerals of the coal are dominated by vitrinite, with a content of 67.24−86.43%, inertinite content ranges from 15.37 to 32.76%, and liptinite macerals are unrecognizable. The vitrinite is mainly composed of telocollinite, followed by desmocollinite, with a small

https://doi.org/10.1021/acsomega.2c00371
ACS Omega 2022, 7, 17063−17074

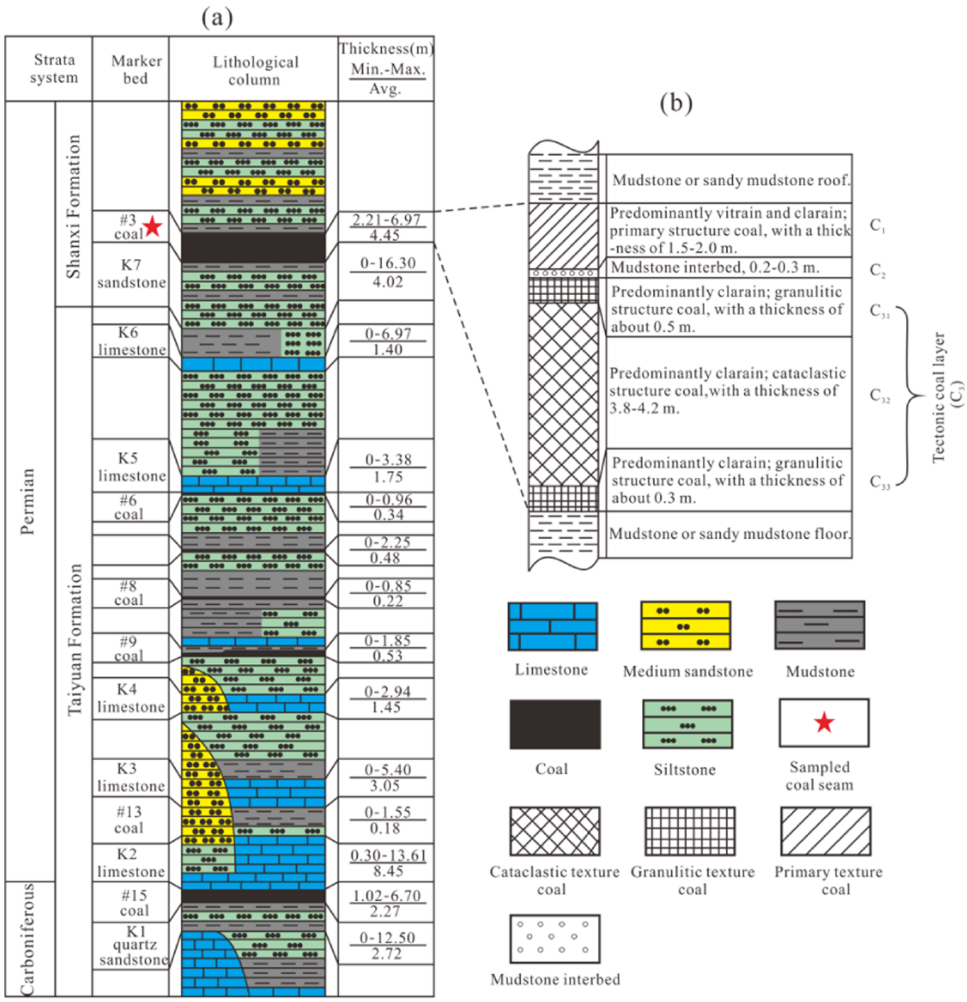

Figure 2. (a) Composite stratigraphic column showing Carboniferous−Permian coal-bearing strata in the Daning block (modified from ref 1, Copyright (2021), with permission from ACS Omega) and (b) column diagram of the No. 3 coal seam.

amount of telinite. The inertinite mainly consists of fusinite, followed by inertodetrinite and macrinite, with a little micrinite. The minerals mainly consist of clay minerals (1.73−14.34%) and calcite (0.22−5.06%), with a small amount of quartz and pyrite.

The No. 3 coal seam is stable and mineable in the whole block, with a thickness of 2.21−6.97 m, averaging 4.45 m. The thick coal seams occur in the northeast and western parts of the block, with a thickness generally over 5 m; while the central part and western border areas host thin coal seams, with a thickness mostly ranging from 2.5 to 4.0 m (Figure 3). The immediate roof is siltstone and mudstone, and the main roof is generally sandstone; the immediate floor is generally siltstone or mudstone (Figure 2a). The No. 3 coal seam is commonly hard at the top and soft at the bottom. From the top to the bottom, the No. 3 coal seam can be divided into three layers, i.e., the primary structure coal layer (C_1), mudstone interbed layer (C_2), and tectonic coal layer (C_3), respectively (Figure 2b). The primary structure coal (1.5−2.0 m) C1 is blocky, with great hardness and a good integrality in the structure; the macroscopic lithotype mainly consists of vitrain and clarain; horizontal beddings are well developed in this layer. The layer of mudstone interbed (C_2) with a thickness of 0.2−0.3 m is commonly underlying the C_1. The tectonic coal layer (C_3) can be further subdivided into three sublayers, including two granulitic structure coal layers (C_{31} and C_{33}) at the upper and lower ends and a cataclastic structure coal layer (C_{32}) in the middle; C_{32} possesses a much larger thickness, with a value of 3.8−4.2 m, and C_{31} and C_{33} are thinner, with a thickness of about 0.5 and 0.3 m, respectively. The tectonic coal in C3 mainly consists of clarain. The tectonic coal was formed after the intact coal was subjected to long-term intense squeezing, shearing, and deformation.[33] The coal seams in the study area were affected by the regional tectonic−thermal evolution in the Mesozoic and Cenozoic, and had experienced multi-stage tectonic stress field effects of compression−extension−compression, resulting in multi-stage tectonic deformations with different directions, properties, and intensities.[34,35] The tectonic coal layer (C_3) in this study area may be formed in these tectonic deformations. Under the influence of tectonic stress, the coal seam not only folds and fractures along with the surrounding rocks but also slides along the bedding to varying degrees when the coal seam is bent and deformed. The sliding surface can appear between the coal seam and the roof, causing the top seam to break up into tectonic coal; it can also appear in the middle of the coal seam, causing the middle seam to break up into tectonic coal; it can also occur at the bottom of the coal seam, causing the bottom seam to break up into tectonic coal.[36] The No. 3 coal seam in the SQB generally

https://doi.org/10.1021/acsomega.2c00371
ACS Omega 2022, 7, 17063−17074

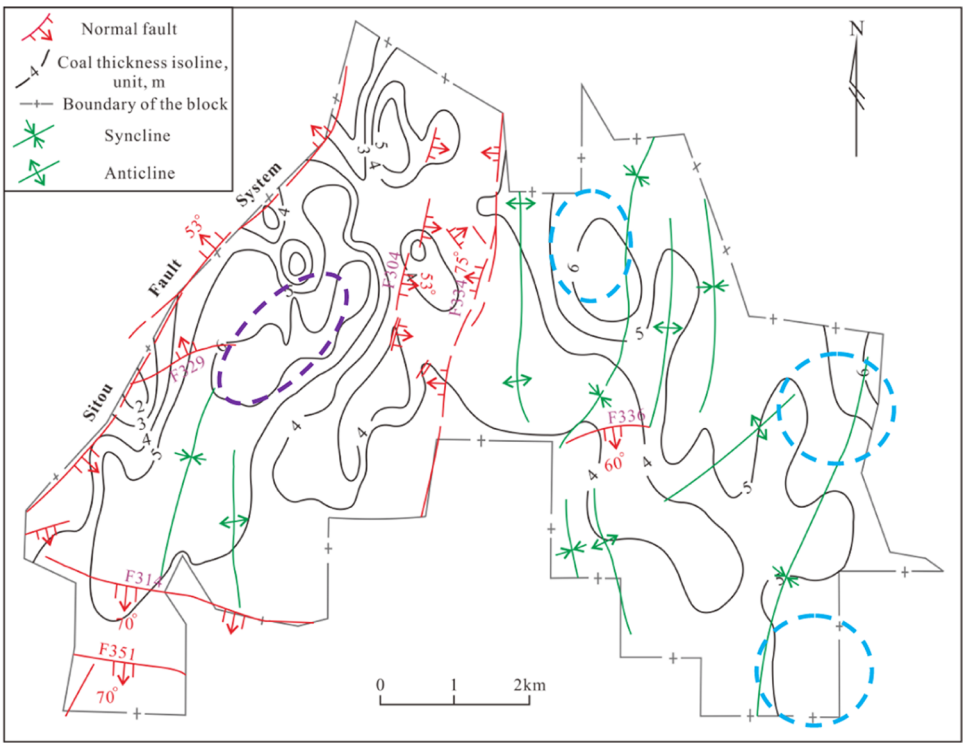

Figure 3. Thickness contour map of the No. 3 coal seam in the Daning block.

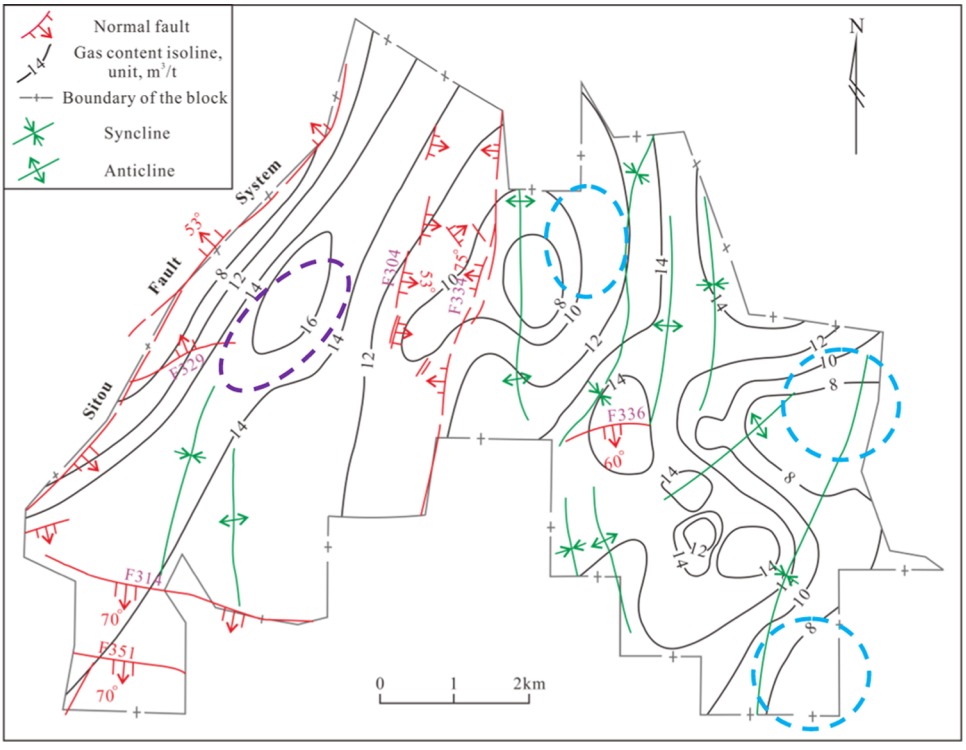

Figure 4. Gas content contour map of the No. 3 coal seam in the Daning block. (modified from ref 1, Copyright (2021), with permission from ACS Omega).

develops tectonic coal in the different parts of the vertical direction.[37−39]

The burial depth of the No. 3 coal seam is approximately 100−600 m. The well testing reservoir pressure ranges from 0.67 to 3.19 MPa, averaging 1.62 MPa. The reservoir pressure gradient ranges from 0.15−0.82 MPa/100m, averaging 0.43 MPa/100m, indicating that this coal seam is an under-pressured reservoir. The well testing permeability ranges from 0.10−6.49 mD, averaging 0.96 mD.

The gas content on the dry, ash-free basis (G_{daf}) of this seam varies from 5.56 to 17.57 m^3/t, averaging 12.83 m^3/t. Overall, the gas content in the western part is higher than that in the

https://doi.org/10.1021/acsomega.2c00371
ACS Omega 2022, 7, 17063−17074

Table 1. Properties and Adsorption Isotherms Parameters of the Coal Samples from the Daning Block[a]

		maceral and mineral (vol %)					Proximate analysis (wt %)					
coal samples	drill ID	V	I	L	M	$R_{o,max}$ (%)	M_{ad}	A_d	V_{daf}	FC_{ad}	$V_{L,ad}$ (cm^3/g)	P_L (MPa)
DN-1	DP-1	63.4	26.2	0	10.4	3.35	1.36	12.99	7.08	79.73	48.46	1.05
DN-2		69.5	25.1	0	5.4	3.11	0.87	18.52	8.70	73.92	54.46	1.32
DN-3	DP-8	70.4	22.3	0	7.3	3.35	1.28	30.21	10.48	62.07	56.45	1.96
DN-4		56.8	32.6	0	10.6	3.36	1.42	26.35	10.07	65.47	42.80	0.97
DN-5	DP-11	61.2	17.6	0	21.2	3.33	1.72	14.77	8.54	76.68	49.19	1.02

[a] $R_{o,max}$ = the maximum vitrinite reflectance; V = vitrinite; I = inertinite; L = liptinite; M = mineral; M_{ad} = moisture (air-dried basis); A_d = ash yield (dry basis); V_{daf} = volatile matter (dry, ash-free basis); FC_{daf} = Fixed carbon (air-dried basis); $V_{L,ad}$ = Langmuir volume (air-dried basis); P_L = Langmuir pressure.

eastern part (Figure 4). The gas content in the parts near the eastern and western borders is generally lower than 8 m^3/t. In addition, the No. 3 coal seam that is near the fault commonly has a lower gas content.

3. SAMPLES AND EXPERIMENTS

The data, such as the coal thickness, $R_{o,max}$, burial depth of coal seam, in situ gas content, and coal quality, were obtained during the CBM exploration and development in the Daning block. The fracturing pressure (p_f), closing pressure (p_c), the pore pressure of the coal seam (p_0), and permeability were obtained through injection/falloff well testing of CBM wells.

In addition, a total of five fresh core samples were collected from the drill holes of CBM wells in the study area. Subsequently, the samples were sealed with black polythene bags immediately and then sent to the laboratory for further analysis. The samples were prepared by crushing and sieving to different particle sizes (<18 mesh, 60−80 mesh, and 200 mesh) for different experiments. Samples with particle sizes smaller than 18 mesh were used to carry out maceral identification and vitrinite reflectance measurements using a Leitz MPV-3 photometer microscope, following the Chinese standards of GB/T 8899-2013 and GB/T 6948-2008, respectively.[40,41] Proximate analysis was conducted on the samples with particle sizes of 200 mesh, using a 5E-MAC infrared fast core analyzer and according to the Chinese standard GB/T 212−2008.[42,43] Samples with particle sizes of 60−80 mesh were used for the methane isothermal adsorption isotherm experiments using an ISO-300 isothermal adsorption apparatus following the Chinese standard GB/T 19560−2008.[39] The test results including coal composition, vitrinite reflectance, proximate analysis, and adsorption isotherms are listed in Table 1.

4. GEOLOGICAL CONTROLS OF THE GAS CONTENT

4.1. Coal Quality. Coal properties, such as ash yield, moisture content, and maceral type, are important factors affecting the adsorption, desorption and, therefore, the total gas content of coal seams.[19] The gas adsorption capacity of coal is also an important factor for gas content because it affects the adsorption and retention of methane over time.[19]

4.1.1. Ash Yield and Moisture Content. The mineral matters (ash) of coals are generally regarded as diluents without sorbing capacity,[44−46] because almost all of the gas in a coal seam is adsorbed on the coal surfaces rather than ash layers or scattered minerals in the coal seam.[19] Therefore, the ash yield reduces the gas storage capacity of coals. Minerals filling in highly metamorphic coals are presented in the crystalline form,[26,47] which occupy the effective pore and fracture spaces in the coal, thus affecting the coals' adsorption capability.[44] From the adsorption isotherms of coals in the Daning block (Figure 5), it can be seen that the adsorption

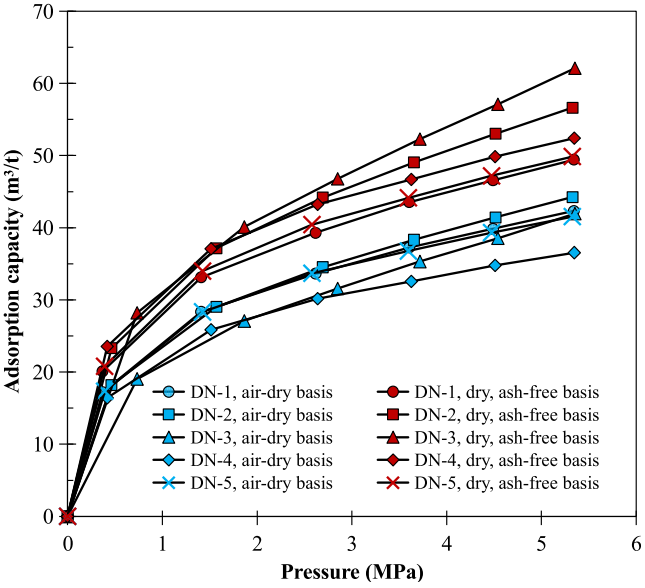

Figure 5. Adsorption isotherms of coals in the Daning block.

capability of coals on a dry, ash-free (daf) basis is obviously higher than that on an air-dried (ad) basis at the same pressure, reflecting the effects of ash yield on adsorption capability of coals. The gas content of coal seams in the Daning block generally decreases with an increase in the ash yield (Figure 6a), which is consistent with previous studies.[15,22,48] The moisture in coals inhibits methane adsorption and storage by competing for adsorption spaces on the coal surface with methane and prevents methane from entering the micropores, and consequently, it reduces the gas content of coals.[44,49−51] The adsorption capacity of coals can decrease significantly with increasing moisture content.[19] In this study, a negative relationship between the gas content of coal seams and moisture content in coals was observed (Figure 6b). The moisture content in coal is affected by the degree of metamorphism of the coal.[52] As mentioned above, the $R_{o,max}$ of coals in the Daning block varies from 2.95 to 3.36%, indicating a high degree and small changes in the metamorphism of the coals, and it causes low moisture contents of coals in the Daning block and relatively small changes. It may be the reason why the moisture content shows an extremely low correlation with the gas content of coals in the Daning block.

https://doi.org/10.1021/acsomega.2c00371
ACS Omega 2022, 7, 17063−17074

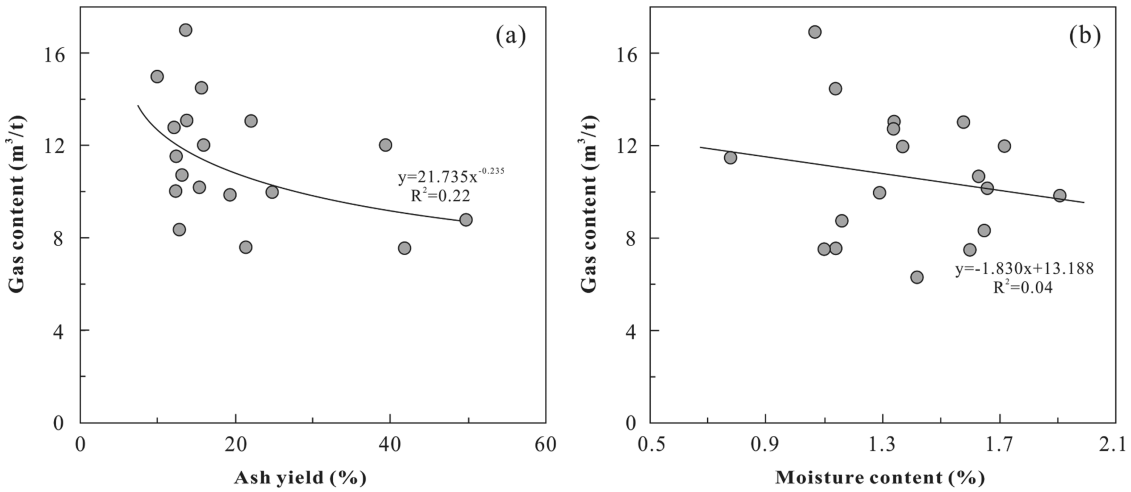

Figure 6. Relationship between ash yield (a) and moisture content (b) with the gas content of coal seams in the Daning block.

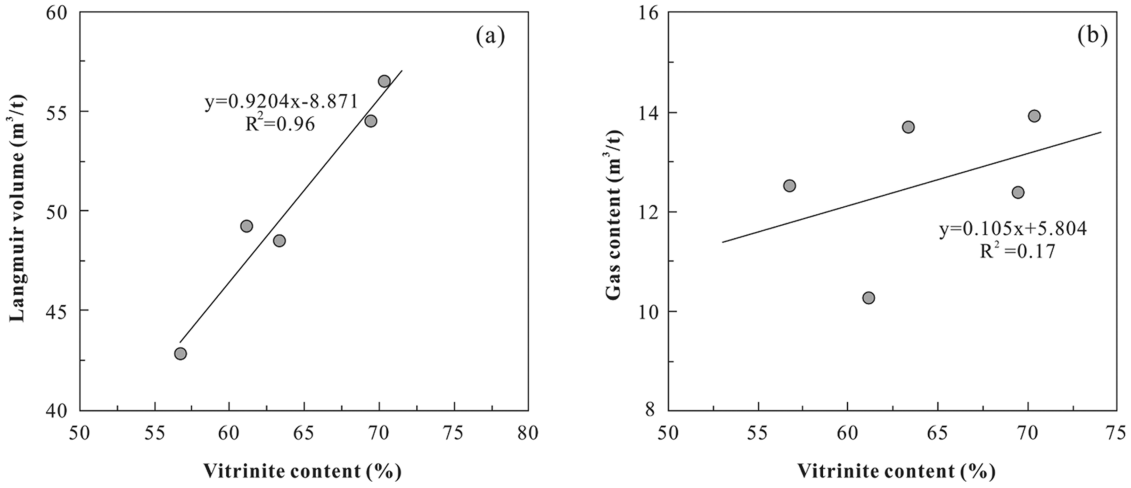

Figure 7. Relationships of vitrinite content with the Langmuir volume (a) and gas content (b) of coal seams in the Daning block.

4.1.2. Maceral Compositions and Gas Adsorption Capacity. The effects of maceral compositions on the gas content are mainly due to the differences in their pore structure and adsorption capacity.[19,45,53−55] Vitrinite-rich coals have a greater adsorption capacity than inertinite-rich coals in most cases,[45,56−59] thereby hosting more gas. Liu et al.[55] suggested that the adsorption capacity of macerals is not fixed but changeable with the increase of coal rank; for low-rank coal, the adsorption capacity of vitrinite is weaker than that of inertinite, and vice versa for high-rank coals. Shen et al.[54] demonstrated that volumes of micropores increase with the increase of vitrinite content, leading to the increase of the specific surface area of coals, thus enhancing the methane adsorption capacity and in situ gas content of coal seams. The maceral compositions of the anthracite studied are dominated by vitrinite, with a content of 67.24−86.43%. As shown in Figure 7a, the vitrinite content of coals has a strong positive correlation with the Langmuir volume, reflecting that the vitrinite-rich coals have a greater gas adsorption capacity than inertinite-rich coals, consequently, the gas content of coals tends to increase with the increase of the vitrinite content, but the correlation is only weakly positive as reflected by the correlation coefficient value (Figure 7b).

As mentioned in the introduction section, the gas content in a coal seam is influenced by multiple geological factors and reservoir conditions, such as burial depth, coal rank, coal thickness, coal quality, sealing conditions, hydrogeology, structural conditions, etc. The relationships between the coal quality (such as ash yield, moisture content, and vitrinite content in this section) and the gas content of the coals presented in this study suggest that coal quality is not the dominant factor influencing the gas content of coals in the Daning block.

4.2. Burial Depth and Coal Thickness. The burial depth in this study refers to the current burial depth of the coal seams, that is, the thickness of the overlying strata, which generally influences the gas content of coal seams.[18,19,22,26,60] The burial depth of a coal seam has a dual effect on gas adsorption.[14,61−63] One is the positive effect of formation pressure, that is, as the burial depth increases, the formation pressure increases, which is conducive to gas adsorption, thus increasing the gas content of the coal seam. The other is the negative effect of strata temperature, that is, as the burial depth increases, the strata temperature increases, leading to a relative decrease in adsorbed gas, thereby reducing the gas content of the coal seam. Therefore, a concept named "critical depth" of coal seams was proposed.[14,61−63] In this study, the strength of the positive effect of formation pressure on the gas content of a coal seam is defined as F_P, and the strength of the negative effect of strata temperature on the gas content of a coal seam is

https://doi.org/10.1021/acsomega.2c00371
ACS Omega 2022, 7, 17063−17074

defined as T_N. When the burial depth is shallower than the critical depth, $F_P > T_N$, the gas content of the coal seam increases with the burial depth, on the contrary, when $F_P < T_N$, the gas content decreases with the burial depth. Therefore, the critical depth of a coal seam refers to the burial depth at which the F_P is equal to the T_N. The gas content of a coal seam is the highest at the critical depth. In this study, the gas content of the No. 3 coal seam demonstrates a relatively strong positive relationship with the burial depth (Figure 8), reflecting that the burial depth of this coal seam in the study area does not reach the critical depth of the Qinshui Basin, which is around 700–750 m.[14,63]

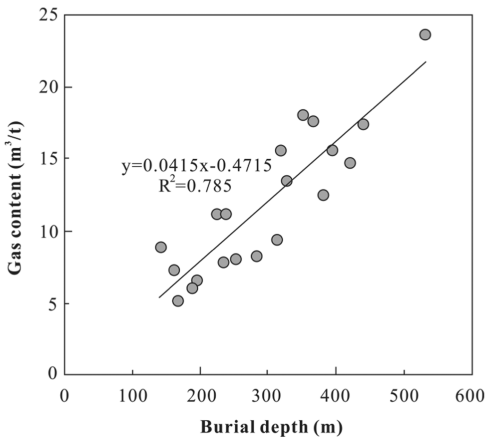

Figure 8. Plots of gas content versus present-day burial depth of the No. 3 coal seam in the Daning block.

Coal beds are both the source rock and the reservoir rock for CBM.[64−66] The coal thickness variation is closely linked with depositional setting and tectonic activities, which have strong influences on the distribution and migration pathways of CBM.[19,22,67,68] The CBM mainly exists on the micropore surface of the coal matrix in the adsorbed state.[69,70] Due to the drop of reservoir pressure of the coal seam or the increase of the temperature of the coal seam, etc., the adsorption capacity of coal for gas weakens. Then the adsorbed CBM is desorbed and accumulated in the microstructures,[71] generating a pressure gradient that leads to CBM escape by diffusion[72,73] and viscous flow.[74−76] The escape of CBM is mainly controlled by the coal permeability[76] and concentration gradient of the gas phase.[75] Wei et al.[77] demonstrated that the greater the coal seam thickness, the longer it will take to reach the median concentration or the end of diffusion. In addition, the coalbed itself is a relatively compact and low-permeability reservoir,[78−80] causing the upper and lower layers of the coalbed to have a sealing effect on the middle layer. The greater the thickness of the coalbed, the longer the gas diffusion path in the middle layer to the roof and floor of the coalbed, and the longer the duration of gas diffusion, which is more favorable to the preservation of CBM during geological history.[81] This may be the fundamental reason for the fact that the coal thickness has a positive correlation with the gas content in a number of coal fields.

In this study, the influence of coal thickness on the gas content of the coal seam can be discussed using the contour maps of coal thickness (Figure 3) and gas content of the coal seam (Figure 4). In some areas of the block, it can be observed that the larger the coal thickness, the higher the gas content of the coal seam. For example, in the western part of the block (Figures 3 and 4), the coal thickness inside the purple dotted line area is commonly larger than 6 m, and correspondingly the gas content is higher than 14 m^3/t, even higher than 16 m^3/t; while the thickness of the coal seam that is near the Sitou fault system is commonly lower than 4 m, and correspondingly the gas content is generally lower than 12 m^3/t. However, in some other areas of the block, though the coal thickness is large, the gas content of the coal seam is low. For example, the coal thickness inside the blue dotted line areas is large (Figures 3 and 4), however, the gas content is generally lower than 10 m^3/t, and even lower than 8 m^3/t. Thus, in terms of the entire block, the overall gas content seems to have a poor correlation with the coal thickness. This may be due to the relatively small change in the thickness of the No. 3 coal seam in the Daning

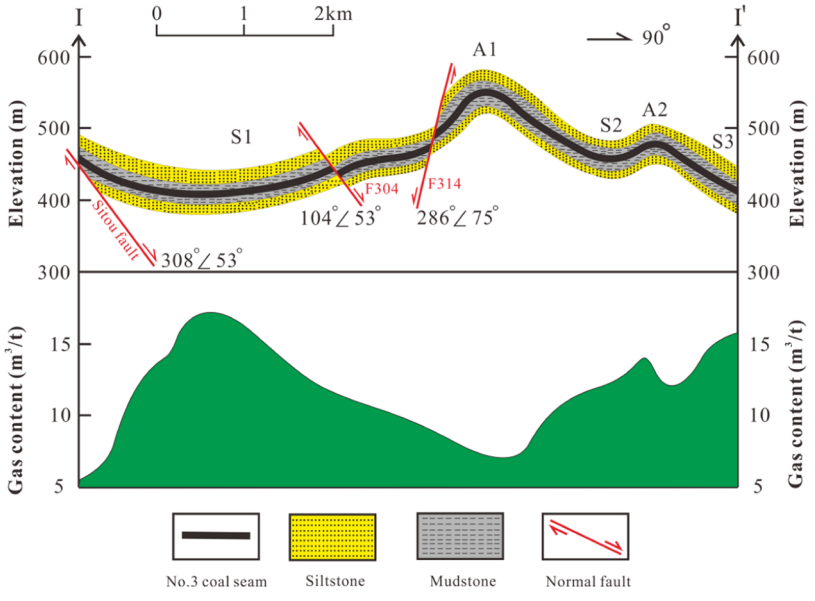

Figure 9. Cross-section I-I′ showing the variation of the gas content of the No. 3 coal seam in different geological structures of the Daning block.

https://doi.org/10.1021/acsomega.2c00371
ACS Omega 2022, 7, 17063−17074

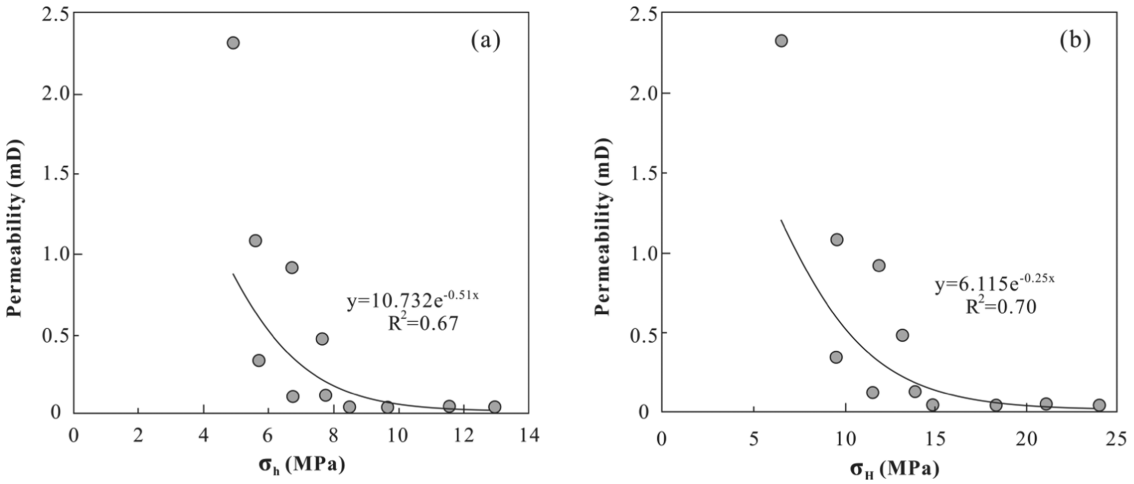

Figure 10. Plots of permeability versus (a) σ_h and (b) σ_H of the coal reservoir in the Daning block.

block, and the impact of coal thickness on the gas content may be concealed by other geological controls.

4.3. Geological Structures. Geological structures with different types have different influences on the preservation and accumulation of CBM in coal reservoirs due to their variable natures under sealing conditions, in situ stress characteristics, hydrodynamic environments, and the continuity of coal seams.[17,18,81,82] The hinge zones of anticlines are found to have more fractures in the strata, resulting in high permeability of the coal seam and the surrounding rocks, which makes the CBM easier to escape through the fractures, so that the gas saturation and gas content of the coal seam are commonly low. In contrast, the hinge zones of synclines usually possess relatively intact rocks, leading to relatively low permeability of coal seam and the surrounding rocks, which is favorable for the preservation of CBM, so that the gas saturation and gas content of coal seams are commonly high.[3,20,65,83]

Faults perform different roles in the process of preservation and accumulation of CBM in the coal reservoir because of their variable properties.[16] On one hand, they may act as channels allowing gas to escape, which leads to a lower gas content in the coalbed; on the other hand, they can serve as obstacles for fluid and gas flow, thus preventing the gas escape and resulting in a higher gas content in the coalbed.[21,22,51,84,85] Previous studies have shown that the reverse faults are commonly favorable for CBM retainment because they have a good seal to prevent the gas from escaping,[20,86,87] whereas the normal faults are generally not favorable for CBM preservation due to bad closure that allows gas to escape.[83,88] In addition, in some cases, both types of faults allow gas to escape irrespective of lithology.[89]

A series of secondary synclines and anticlines are well developed in the Daning block (Figure 1c). The gas content distribution of coal seam is significantly influenced by these folds. The high gas content areas are mainly distributed along the axial part of the secondary syncline, while some low gas content areas are found along the axial part of the secondary anticline (Figure 4). A series of normal faults are well developed in the western part of the study area, and coal seams near these faults are usually low in gas content (Figure 4). For example, the gas content of coal seams near the Sitou fault system on the west side of the study area is usually less than 8 m^3/t; coal seams near the F334 fault in the central part also have a relatively lower gas content of 8−10 m^3/t. Figure 9 shows a W−E cross-section I-I′ in Figure 1c. In the section, the highest gas content of the coal seam appears at the hinge zone of the S1 secondary syncline, and the gas content shows a decreasing trend from the hinge zone to the two limbs. The lowest gas content of a coal seam occurs at the hinge zone of the A1 secondary anticline, and the gas content presents an increasing trend from the hinge zone to the two limbs. The coal seams in hinge zones S2 and S3 secondary synclines have high values of gas content, whereas the gas content of the coal seams in hinge zone A2 secondary anticline between S2 and S3 is relatively low. The coal seam near the Sitou fault has an extremely low gas content in the section, and the gas content gradually increases as the distance between the coal seam and the fault increases (Figure 9), indicating that the Sitou fault has a negative effect on the CBM preservation in the Daning block. The gas content of the coal seam between faults F304 and F314 is relatively low in the section (Figure 9), implying that the two fault systems allow the gas to escape.

5. GEOLOGICAL CONTROLS OF PERMEABILITY

Based on the well testing permeability data of coal reservoirs in the Daning block, it was found that the coal permeability in this area is generally above 0.1 mD, with an average value of 0.96 mD, which is higher than most of the CBM production blocks in China.[28] In this study, the factors of in situ stress, burial depth, and coal structure on the permeability of coals in the Daning block were discussed.

5.1. In Situ Stress. In situ stress is a key factor affecting the permeability of coal reservoirs, because it controls the fracture space structure by determining the density, direction, and closure and opening degree of fractures in the coal reservoirs.[90−92] The permeability of coal is extremely sensitive to in situ stress and generally decreases exponentially with the increase of in situ stress.[23,27,93]

The fracturing pressure (p_f), closing pressure (p_c), pore pressure of the coal seam (p_0), and permeability were obtained through injection/falloff well testing. The maximum horizontal principal stress (σ_H) can be expressed as eq 1.[94]

$$\sigma_H = 3p_c - p_f - p_0 + T \quad (1)$$

where σ_H is the maximum horizontal principal stress, MPa; p_c is the closing pressure, MPa; p_f is the fracturing pressure, MPa; p_0 is the pore pressure of the coal seam (initial reservoir

https://doi.org/10.1021/acsomega.2c00371
ACS Omega 2022, 7, 17063−17074

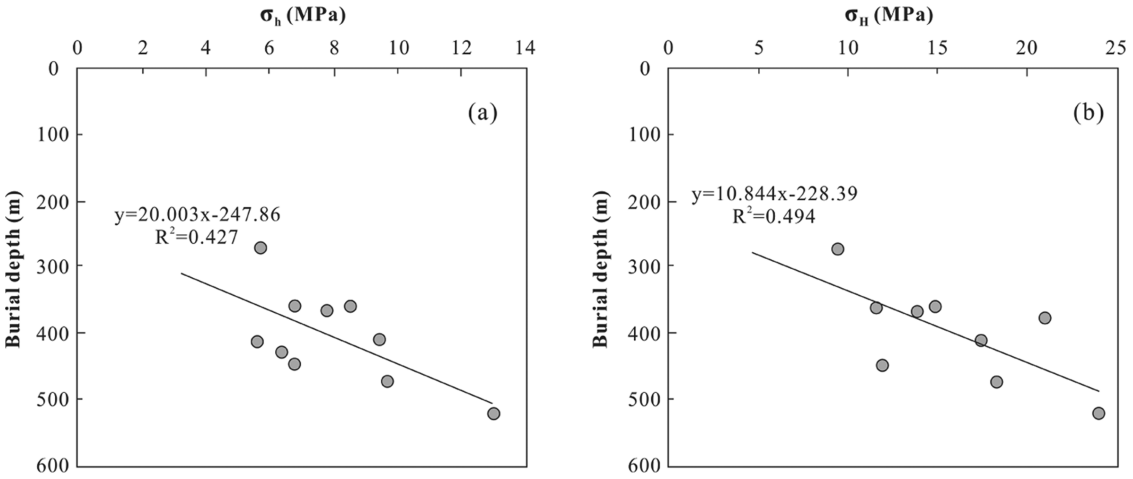

Figure 11. Plots of burial depth versus (a) σ_h and (b) σ_H of the coal reservoir in the Daning block.

pressure), MPa; and T is the tensile strength of the rock around the borehole, MPa.

The equilibrium pressure just enough to keep the fracture open is called closing pressure (p_c), which is equivalent to the minimum horizontal principal stress (σ_h) perpendicular to the fracture surface,[95,96] i.e.

$$\sigma_h = p_c \quad (2)$$

Based on the well testing interpretation, the well testing permeability of coal reservoirs in the Daning block also decreases exponentially with the increase of in situ horizontal stresses (Figure 10). The functional relations between permeability (K) and in situ horizontal stresses are expressed as follows

$$K = 10.732 \times e^{-0.51\sigma_h} \quad (3)$$

$$K = 6.115 \times e^{-0.25\sigma_H} \quad (4)$$

Figure 10 shows that when the minimum horizontal stress (σ_h) is higher than 8 MPa, high permeability data disappear. In addition, when the maximum horizontal principal stress (σ_H) is higher than 15 MPa, the permeability is extremely low in the Daning block. The above phenomena indicate a dominant impact of in situ stress on the coal permeability in the Daning block.

5.2. Burial Depth. In situ stress commonly tends to increase with the increase of the burial depth of the coal seam. Since in situ stress generally has a negative effect on the permeability of coal seams, therefore, the permeability of coal seams generally decreases as the burial depth increases.[91,92] In this study area, both σ_h and σ_H increase with an increase in the burial depth of coal seams (Figure 11). Thus, as shown in Figure 12, the permeability of coal reservoirs in the Daning block decreases at an exponential function with the increase of the burial depth of the coal seam, i.e.

$$K = 2.3295 \times e^{-0.0084D} \quad (5)$$

where K is the permeability of the coal seam, mD and D is the burial depth of the coal seam, m.

5.3. Coal Structure. The permeability of coal reservoirs is largely dependent on the coal structure under in situ conditions.[25] The coal structure is the product of coal deformation under tectonic stress,[33,97] and it is an indirect reflection of coal permeability. Based on the distinguishable

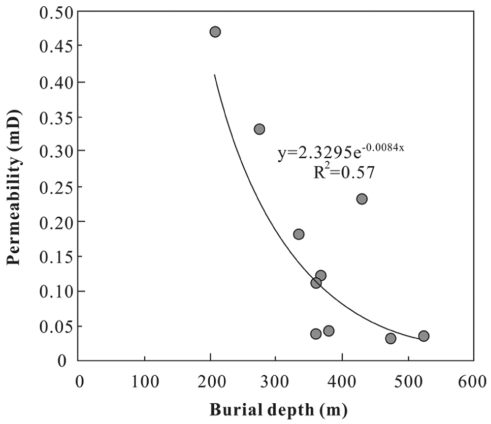

Figure 12. Relationship between permeability and burial depth of the No. 3 coal seam in the Daning block.

degree of coal macrolithotype, coal-body damage degree, fracture and corrugation development degree, and hand-test strength, the coal structure is simply divided into four types, i.e., primary structure (or undeformed), cataclastic structure, granulitic structure, and mylonitic structure.[37,98] The last three types are collectively called tectonic coal.[99] The field permeability of tectonic coal is commonly obviously lower than that of primary coal.[33] In this area, nearly all of the CBM wells require hydro-fracturing stimulation technology to enhance the coal permeability.[1] Compared with granulitic and mylonitic structure coals, the primary and cataclastic structure coals have a complete coal-body structure and high strength, leading to a good hydro-fracturing potential.[81] In this area, the field experiences indicate that the greater proportion of the primary structure coal layer (C_1) and cataclastic structure coal layer (C_{32}) in the total coal thickness (Figure 2b), the higher the permeability of the coal seam through hydro-fracturing.

6. CONCLUSIONS

(1) The coal reservoirs in the Daning block of SQB have great potential for CBM production. Coal rank in the Daning block is anthracite. The gas content ranges from 5.56 to 17.57 (avg. 12.83) m^3/t, and the coal permeability is generally above 0.1 mD, with an average of 0.96 mD.

https://doi.org/10.1021/acsomega.2c00371
ACS Omega 2022, 7, 17063−17074

(2) The gas content of coal reservoirs in the Daning block shows very weak positive correlations with ash yield, moisture content, and vitrinite content, indicating that the coal quality is not the dominating factor influencing the gas content of coal reservoirs in the Daning block. The gas content presents a strong positive correlation with the burial depth of a coal seam, but poorly correlates with the coal thickness. The CBM enrichment areas are generally located in the axial part of secondary syncline, while the lower gas content areas commonly occur at the axial part of secondary anticline. The gas content of coal seams that are near the normal faults is commonly lower.

(3) In situ stress has the dominant impact on the coal permeability in the Daning block. The well testing permeability of coal reservoirs decreases exponentially with the increases of the minimum horizontal stress (σ_h) and the maximum horizontal principal stress (σ_H). With the increase in the burial depth of the coal seam, the coal permeability also decreases exponentially. The primary and cataclastic structure coals generally have higher hydro-fracturing permeability than the granulitic and mylonitic structure coals.

AUTHOR INFORMATION

Corresponding Author

Zheng Zhang − *Key Laboratory of Coalbed Methane Resources and Reservoir Formation Process, Ministry of Education, China University of Mining and Technology, Xuzhou, Jiangsu 221008, China;* orcid.org/0000-0003-2042-7741; Email: zhangzheng@cug.edu.cn

Authors

Zhiqi Guo − *Key Laboratory of Coalbed Methane Resources and Reservoir Formation Process, Ministry of Education, China University of Mining and Technology, Xuzhou, Jiangsu 221008, China*

Yunxing Cao − *School of Safety Science and Engineering, Henan Polytechnic University, Jiaozuo 454003, China*

Shi Dong − *Shanxi Lanhua Sci-tech Venture Co., Ltd., Jincheng 048000, China*

Complete contact information is available at: https://pubs.acs.org/10.1021/acsomega.2c00371

Notes

The authors declare no competing financial interest.

ACKNOWLEDGMENTS

This work was financially supported by the Science and Technology Key Special Project of Shanxi Province (No. 20111101003) and the Natural Science Foundation of China (No. 41802192).

REFERENCES

(1) Guo, Z.; Cao, Y.; Dong, S.; Zhang, Z. Experimental studies on the enhancement of permeability of anthracite by acidizing: a case study in the Daning block, Southern Qinshui Basin. *ACS Omega* **2021**, *6*, 31112−31121.

(2) Li, X.; Zhang, J.; Li, C.; Chen, W.; He, J.; Zheng, Y.; Li, R. Characteristic law of borehole deformation induced by the temperature change in the surrounding rock of deep coalbed methane well. *J. Energy Resour. Technol.* **2022**, *144*, No. 063003.

(3) Moore, T. A. Coalbed methane: a review. *Int. J. Coal Geol.* **2012**, *101*, 36−81.

(4) Hamawand, I.; Yusaf, T.; Hamawand, S. G. Coal seam gas and associated water: A review paper. *Renewable Sustainable Energy Rev.* **2013**, *22*, 550−560.

(5) Qin, Y.; Moore, T. A.; Shen, J.; Yang, Z.; Shen, Y.; Wang, G. Resources and geology of coalbed methane in China: a review. *Int. Geol. Rev.* **2018**, *60*, 777−812.

(6) Karimpouli, S.; Tahmasebi, P.; Ramandi, H. L. A review of experimental and numerical modeling of digital coalbed methane: Imaging, segmentation, fracture modeling and permeability prediction. *Int. J. Coal Geol.* **2020**, *228*, No. 103552.

(7) Qin, Y.; Shen, J.; Shi, R. Strategic Value and Choice on Construction of CMG Industry in China. *J. China Coal Soc.* **2021**, *47*, 371−387.

(8) Xu, F.; Xiao, Z.; Chen, D.; Yan, X.; Wu, N.; Li, X.; Miao, Y. Current status and development direction of coalbed methane exploration technology in China. *Coal Sci. Technol.* **2019**, *47*, 205−215.

(9) Luo, D.; Dai, Y.; Xia, L. Economic evaluation based policy analysis for coalbed methane industry in China. *Energy* **2011**, *36*, 360−368.

(10) Jianchao, H.; Wang, Z.; Liu, P. Current states of coalbed methane and its sustainability perspectives in China. *Int. J. Energy Res.* **2018**, *42*, 3454−3476.

(11) Zhang, Z.; Yan, D.; Yang, S.; Zhuang, X.; Li, G.; Wang, G.; Wang, X. Experimental studies on the movable-water saturations of different-scale pores and relative permeability of low-medium rank coals from the Southern Junggar Basin. *J. Nat. Gas Sci. Eng.* **2020**, *83*, No. 103585.

(12) Liang, W.; Yan, J.; Zhang, B.; Hou, D. Review on coal bed methane recovery theory and technology: recent progress and perspectives. *Energy Fuels* **2021**, *35*, 4633−4643.

(13) Tao, S.; Pan, Z.; Tang, S.; Chen, S. Current status and geological conditions for the applicability of CBM drilling technologies in China: A review. *Int. J. Coal Geol.* **2019**, *202*, 95−108.

(14) Song, Y.; Liu, S.; Ju, Y.; Hong, F.; Jiang, L.; Ma, X.; Wei, M. Coupling between gas content and permeability controlling enrichment zones of high abundance coal bed methane. *Acta Pet. Sin.* **2013**, *34*, 417−426.

(15) Liu, H.; Sang, S.; Wang, G. G. X.; Li, Y.; Li, M.; Liu, S. Evaluation of the synergetic gas-enrichment and higher-permeability regions for coalbed methane recovery with a fuzzy model. *Energy* **2012**, *39*, 426−439.

(16) Lv, Y.; Tang, D.; Xu, H.; Luo, H. Production characteristics and the key factors in high-rank coalbed methane fields: a case study on the Fanzhuang Block, Southern Qinshui Basin, China. *Int. J. Coal Geol.* **2012**, *96*−*97*, 93−108.

(17) Pashin, J. C. Stratigraphy and structure of coalbed methane reservoirs in the United States: an overview. *Int. J. Coal Geol.* **1998**, *35*, 209−240.

(18) Ayers, W. B., Jr. Coalbed gas system, resources, and production and a review of contrasting cases from the San Juan and Powder River basins. *AAPG Bull.* **2002**, *86*, 1853−1890.

(19) Scott, A. R. Hydrogeologic factors affecting gas content distribution in coal beds. *Int. J. Coal Geol.* **2002**, *50*, 363−387.

(20) Chen, Y.; Tang, D.; Xu, H.; Li, Y.; Meng, Y. Structural controls on coalbed methane accumulation and high production models in the eastern margin of Ordos Basin, China. *J. Nat. Gas Sci. Eng.* **2015**, *23*, 524−537.

(21) Zhang, J.; Liu, D.; Cai, Y.; Pan, Z.; Yao, Y.; Wang, Y. Geological and hydrological controls on the accumulation of coalbed methane within the No. 3 coal seam of the southern Qinshui Basin. *Int. J. Coal Geol.* **2017**, *182*, 94−111.

(22) Esen, O.; Özer, S. C.; Soylu, A.; Rend, A. R.; Fişne, A. Geological controls on gas content distribution of coal seams in the Kınık coalfield, Soma Basin, Turkey. *Int. J. Coal Geol.* **2020**, *231*, No. 103602.

(23) McKee, C. R.; Bumb, A. C.; Koenig, R. A. Stress-dependent permeability and porosity of coal and other geologic formations. *SPE Form. Eval.* **1988**, *3*, 81−91.
(24) Clarkson, C. R.; Bustin, R. M. Variation in permeability with lithotype and maceral composition of Cretaceous coals of the Canadian Cordillera. *Int. J. Coal Geol.* **1997**, *33*, 135−151.
(25) Fu, X.; Qin, Y.; Wang, G. G. X.; Rudolph, V. Evaluation of coal structure and permeability with the aid of geophysical logging technology. *Fuel* **2009**, *88*, 2278−2285.
(26) Cai, Y.; Liu, D.; Yao, Y.; Li, J.; Qiu, Y. Geological controls on prediction of coalbed methane of No. 3 coal seam in Southern Qinshui Basin, North China. *Int. J. Coal Geol.* **2011**, *88*, 101−112.
(27) Meng, Z.; Zhang, J.; Wang, R. In-situ stress, pore pressure, and stress-dependent permeability in the southern Qinshui Basin. *Int. J. Rock Mech. Min.* **2011**, *48*, 122−131.
(28) Ye, J.; Shi, B.; Zhang, C. Coal reservoir permeability and its controlled factors in China. *J. China Coal Soc.* **1999**, *24*, 118−122.
(29) Liu, C.; Zhu, Z. Technical status and key developing points of coal-bed methane industry in Shanxi Province. *Shanxi Sci. Technol.* **2020**, *35*, 11−14.
(30) Zhao, X.; Zhu, Q.; Sun, F.; Yang, Y.; Wang, B.; Zuo, Y.; Shen, J.; Mu, F.; Li, M. Practice and thought of coalbed methane exploration and development in Qinshui Basin. *J. China Coal Soc.* **2015**, *40*, 2131−2136.
(31) Zhang, Z.; Qin, Y.; Bai, J.; Li, G.; Zhuang, X.; Wang, X. Hydrogeochemistry characteristics of produced waters from CBM wells in Southern Qinshui Basin and implications for CBM commingled development. *J. Nat. Gas Sci. Eng.* **2018**, *56*, 428−443.
(32) Ren, Z.; Xiao, H.; Liu, L.; Zhang, S.; Qin, Y.; Wei, C. The evidence of fission-track data for the study of tectonic thermal history in Qinshui Basin. *Chin. Sci. Bull.* **2005**, *50*, 104−110.
(33) Cheng, Y.; Pan, Z. Reservoir properties of Chinese tectonic coal: A review. *Fuel* **2020**, *260*, No. 116350.
(34) Wei, M.; Ju, Y.; Xue, C.; Hou, Q. Characteristics of coal reservoirs and division of coalbed methane enrichment areas in the south of Qinshui Basin. *Chin. J. Geol.* **2011**, *46*, 905−918.
(35) Meng, Z.; Liu, S.; Wang, B.; Yu, Z. Study on feature of coal body structure and logging response in Jincheng Mining Area. *Coal Sci. Technol.* **2015**, *43*, 58−63.
(36) Fu, X.; Qin, Y. *Theories and Techniques of Permeability Prediction Of Multiphase Medium Coalbed-methane Reservoirs*, 1st ed.; China University of Mining and Technology Press: Xuzhou, China, 2003; pp. 114−123.
(37) Teng, J.; Yao, Y.; Liu, D.; Cai, Y. Evaluation of coal texture distributions in the southern Qinshui basin, North China: Investigation by a multiple geophysical logging method. *Int. J. Coal Geol.* **2015**, *140*, 9−22.
(38) Yang, G.; Tang, S.; Zhang, S.; Hu, W.; Xi, Z.; Li, L.; Li, Y.; Li, J.; Wang, M.; Gong, M. Impacts of vertical variation of different coal texture types on coalbed methane production in Zaoyuan area of the Shizhuangnan Block, Southern Qinshui Basin, North China. *Energy Sources, Part A* **2017**, *39*, 1617−1624.
(39) Cao, L.; Yao, Y.; Liu, D.; Yang, Y.; Wang, Y.; Cai, Y. Application of seismic curvature attributes in the delineation of coal texture and deformation in Zhengzhuang field, southern Qinshui Basin. *AAPG Bull.* **2020**, *104*, 1143−1166.
(40) GB/T 8899−2013, 2013. *Determination of Maceral Group Composition and Minerals in Coal* (in Chinese).
(41) GB/T 6948−2008, 2008. *Method of Determining Microscopically the Reflectance of Vitrinite in Coal* (in Chinese).
(42) GB/T 212−2008, 2008. *Proximate Analysis of Coal* (in Chinese).
(43) GB/T 19560−2008, 2008. *Experimental Method of High-pressure Adsorption Isothermal to Coal* (in Chinese).
(44) Bustin, R. M.; Clarkson, C. R. Geological controls on coalbed methane reservoir capacity and gas content. *Int. J. Coal Geol.* **1998**, *38*, 3−26.
(45) Crosdale, P. J.; Beamish, B. B.; Valix, M. Coalbed methane sorption related to coal composition. *Int. J. Coal Geol.* **1998**, *35*, 147−158.
(46) Laxminarayana, C.; Crosdale, P. J. Role of coal type and rank on methane sorption characters of Bowen Basin, Australia coals. *Int. J. Coal Geol.* **1999**, *40*, 309−325.
(47) Ward, C. R. Minerals in bituminous coals of the Sydney basin (Australia) and the Illinois basin (U.S.A.). *Int. J. Coal Geol.* **1989**, *13*, 455−479.
(48) Butland, C. I.; Moore, T. A. Secondary biogenic coal seam gas reservoirs in New Zealand: a preliminary assessment of gas contents. *Int. J. Coal Geol.* **2008**, *76*, 151−165.
(49) Crosdale, P. J.; Moore, T. A.; Mares, T. E. Influence of moisture content and temperature on methane adsorption isotherm analysis for coals from a low-rank, biogenically-sourced gas reservoir. *Int. J. Coal Geol.* **2008**, *76*, 166−174.
(50) Warwick, P. D.; Breland, F. C., Jr.; Hackley, P. C. Biogenic origin of coalbed gas in the northern Gulf of Mexico Coastal Plain, U.S.A. *Int. J. Coal Geol.* **2008**, *76*, 119−137.
(51) Hou, S.; Wang, X.; Wang, X.; Yuan, Y.; Zhuang, X.; Wang, X. Geological controls on gas saturation in the Yanchuannan Coalbed Methane Field, Southeastern Ordos Basin, China. *Mar. Pet. Geol.* **2016**, *78*, 254−270.
(52) Chen, J.; Shao, Z.; Qin, Y. *Energy Geology*, 1st ed.; China University of Mining and Technology Press: Xuzhou, China, 2003; pp. 58−60.
(53) Zhang, Q.; Yang, X. Isothermal adsorption of coals on methane under equilibrium moisture. *J. China Coal Soc.* **1999**, *24*, 566−570.
(54) Shen, J.; Qin, Y.; Zhao, J. Maceral contribution to pore size distribution in anthracite in the south Qinshui Basin. *Energy Fuels* **2019**, *33*, 7234−7243.
(55) Liu, L.; Jin, C.; Li, L.; Xu, C.; Sun, P.; Meng, Z.; An, L. Coalbed methane adsorption capacity related to maceral compositions. *Energy Explor. Exploit.* **2020**, *38*, 79−91.
(56) Ettinger, I.; Eremin, I.; Zimakov, B.; Yanovskaya, M. Natural factors influencing coal sorption properties I—Petrography and the sorption properties of coals. *Fuel* **1966**, *45*, 267−275.
(57) Levine, J. R.; Johnson, P. W.; Beamish, B. B. *High Pressure Microbalance Sorption Studies*, Proceedings of the 1993 International Coalbed Methane Symposium, The University of Alabama: Birmingham, USA, 17−21 May 1993; pp. 187−196.
(58) Lamberson, M. N.; Bustin, R. M. Coalbed methane characteristics of Gates Formation coals, Northeastern British Colombia: effect of maceral composition. *AAPG Bull.* **1993**, *77*, 2062−2076.
(59) Zhang, Z.; Qin, Y.; Fu, X.; Wu, C. Distribution law of gas-bearing property of coal seams and analysis on geological control factors in Panzhuang Block. *Coal Sci. Technol.* **2014**, *42*, 98−102.
(60) Yao, Y.; Liu, D.; Tang, D.; Tang, S.; Che, Y.; Huang, W. Preliminary evaluation of the coalbed methane production potential and its geological controls in the Weibei Coalfield, Southeastern Ordos Basin, China. *Int. J. Coal Geol.* **2009**, *78*, 1−15.
(61) Qin, Y.; Shen, J. On the fundamental issues of deep coalbed methane geology. *Acta Pet. Sin.* **2016**, *37*, 125−136.
(62) Chen, S.; Tang, D.; Tao, S.; Zhao, J.; Li, Y.; Liu, W. Discussion about "critical depth" of deep coalbed methane in Zhengzhuang area, Qinshui Basin. *J. China Coal Soc.* **2016**, *41*, 3069−3075.
(63) Shen, J. CBM-reservoiring Effect in Deep Strata, [Dissertation]. China University of Mining and Technology, 2011.
(64) Pashin, J. C. Coal as a Petroleum Source Rock and Reservoir Rock. In *Applied Coal Petrology*, 1st ed.; Suárez-Ruiz, I.; Crelling, J., Eds.; Elsevier, 2008; pp. 227−262.
(65) Song, Y.; Liu, H.; Hong, F.; Qin, S.; Liu, S.; Li, G.; Zhao, M. Syncline reservoir pooling as a general model for coalbed methane (CBM) accumulations: mechanisms and case studies. *J. Pet. Sci. Eng.* **2012**, *88*−*89*, 5−12.
(66) Aminian, K.; Rodvelt, G. Evaluation of Coalbed Methane Reservoirs. In *Coal Bed Methane*, 1st ed.; Thakur, P.; Schatzel, S.; Aminian, K., Eds.; Elsevier, 2014; pp 63−91.

https://doi.org/10.1021/acsomega.2c00371
ACS Omega 2022, 7, 17063−17074

(67) Xu, H.; Tang, D.; Liu, D.; Tang, S.; Yang, F.; Chen, X.; He, W.; Deng, C. Study on coalbed methane accumulation characteristics and favorable areas in the Binchang area, southwestern Ordos Basin, China. *Int. J. Coal Geol.* **2012**, *95*, 1−11.
(68) Cai, Y.; Liu, D.; Zhang, K.; Elsworth, D.; Yao, Y.; Tang, D. Preliminary evaluation of gas content of the No. 2 coal seam in the Yanchuannan area, southeast Ordos basin, China. *J. Pet. Sci. Eng.* **2014**, *122*, 675−689.
(69) Gray, I. Reservoir engineering in coal seams: part 1-The physical process of gas storage and movement in coal seams. *SPE Reservoir Eng.* **1987**, *2*, 28−34.
(70) Karacan, C.Ö.; Okandan, E. Fracture/cleat analysis of coals from Zonguldak Basin (northwestern Turkey) relative to the potential of coalbed methane production. *Int. J. Coal Geol.* **2000**, *44*, 109−125.
(71) Chen, B.; Stuart, F. M.; Xu, S.; Györe, D.; Liu, C. Evolution of coal-bed methane in Southeast Qinshui Basin, China: insights from stable and noble gas isotopes. *Chem. Geol.* **2019**, *529*, No. 119298.
(72) Wei, C.; Qin, Y.; Wang, G. G. X.; Fu, X.; Zhang, Z. Numerical simulation of coalbed methane generation, dissipation and retention in SE edge of Ordos Basin, China. *Int. J. Coal Geol.* **2010**, *82*, 147−159.
(73) Tian, F.-c.; Liang, Y.; Wang, D.; Jin, K. Effects of caprock sealing capacities on coalbed methane preservation: experimental investigation and case study. *J. Cent. South Univ.* **2019**, *26*, 925−937.
(74) Rice, D. D. Composition and origins of coalbed gas. *AAPG Stud. Geol.*, 1993; *38*, 159−184.
(75) Saghafi, A.; Javanmard, H.; Roberts, D. In *Parameters Affecting Coal Seam Gas Escape through Floor and Roof Strata*, Proceedings of the 2010 Underground Coal Operators' Conference, Wollongong, Australia, 11−12 February 2010, Aziz, N.; Aziz, N., Eds.; University of Wollongong: Wollongong, Australia, 2010; pp. 210−216.
(76) Amann-Hildenbrand, A.; Ghanizadeh, A.; Krooss, B. M. Transport properties of unconventional gas systems. *Mar. Pet. Geol.* **2012**, *31*, 90−99.
(77) Wei, C.; Liu, H.; Meng, J. Numerical simulation of coalbed methane diffusion in geohistory. *Coal Geol. Explor.* **1998**, *26*, 19−24.
(78) Pant, L. M.; Huang, H.; Secanell, M.; Larter, S.; Mitra, S. K. Multi scale characterization of coal structure for mass transport. *Fuel* **2015**, *159*, 315−323.
(79) Sampath, K. H. S. M.; Perera, M. S. A.; Elsworth, D.; Ranjith, P. G.; Matthai, S. K.; Rathnaweera, T.; Zhang, G. Effect of coal maturity on CO2-based hydraulic fracturing process in coal seam gas reservoirs. *Fuel* **2019**, *236*, 179−189.
(80) Peng, Z.; Liu, S.; Li, Y.; Yao, Q. Apparent permeability prediction of coal matrix with generalized lattice Boltzmann model considering non-Darcy effect. *Geofluids* **2020**, *2020*, 1−14.
(81) Fu, X.; Qin, Y.; Wei, C. *Coalbed Methane Geology*, 1st ed.; China University of Mining and Technology Press: Xuzhou, China, 2007; pp 98−138.
(82) Tao, S.; Tang, D.; Xu, H.; Gao, L.; Fang, Y. Factors controlling high-yield coalbed methane vertical wells in the Fanzhuang Block, Southern Qinshui Basin. *Int. J. Coal Geol.* **2014**, *134*−*135*, 38−45.
(83) Liu, D.; Yao, Y.; Tang, D.; Tang, S.; Che, Y.; Huang, W. Coal reservoir characteristics and coalbed methane resource assessment in Huainan and Huaibei coalfields, Southern North China. *Int. J. Coal Geol.* **2009**, *79*, 97−112.
(84) Yin, S.; Ding, W. Evaluation indexes of coalbed methane accumulation in the strong deformed strike-slip fault zone considering tectonics and fractures: a 3D geomechanical simulation study. *Geol. Mag.* **2019**, *156*, 1052−1068.
(85) Wang, H.; Yao, Y.; Huang, C.; Liu, D.; Cai, Y. Fault development characteristics and their effects on current gas content and productivity of No.3 coal seam in the Zhengzhuang field, Southern Qinshui Basin, North China. *Energy Fuels* **2021**, *35*, 2268−2281.
(86) Johnson, R. C.; Flores, R. M. Developmental geology of coalbed methane from shallow to deep in Rocky Mountain basins and in Cook Inlet−Matanuska basin, Alaska, U.S.A. and Canada. *Int. J. Coal Geol.* **1998**, *35*, 241−282.
(87) Kinnon, E. C. P.; Golding, S. D.; Boreham, C. J.; Baublys, K. A.; Esterle, J. S. Stable isotope and water quality analysis of coal bed methane production waters and gases from the Bowen Basin, Australia. *Int. J. Coal Geol.* **2010**, *82*, 219−231.
(88) Kędzior, S.; Kotarba, M. J.; Pękała, Z. Geology, spatial distribution of methane content and origin of coalbed gases in Upper Carboniferous (Upper Mississippian and Pennsylvanian) strata in the South-Eastern part of the Upper Silesian Coal Basin, Poland. *Int. J. Coal Geol.* **2013**, *105*, 24−35.
(89) Sośnicka, M.; Lüders, V. Fluid inclusion evidence for low-temperature thermochemical sulfate reduction (TSR) of dry coal gas in Upper Permian carbonate reservoirs (Zechstein, Ca2) in the North German Basin. *Chem. Geol.* **2020**, *534*, No. 119453.
(90) Bachu, S.; Michael, K. Possible controls of hydrogeological and stress regimes on the producibility of coalbed methane in Upper Cretaceous−Tertiary strata of the Alberta basin, Canada. *AAPG Bull.* **2003**, *87*, 1729−1754.
(91) Zhao, J.; Tang, D.; Xu, H.; Li, Y.; Li, S.; Tao, S.; Lin, W.; Liu, Z. Characteristic of In Situ Stress and Its Control on the Coalbed Methane Reservoir Permeability in the Eastern Margin of the Ordos Basin, China. *Rock Mech. and Rock Eng.* **2016**, *49*, 3307−3322.
(92) Ju, W.; Jiang, B.; Qin, Y.; Wu, C.; Wang, G.; Qu, Z.; Li, M. The present-day in-situ stress field within coalbed methane reservoirs, Yuwang Block, Laochang Basin, south China. *Mar. Pet. Geol.* **2019**, *102*, 61−73.
(93) Somerton, W. H.; Söylemezoğlu, I. M.; Dudley, R. C. Effect of stress on permeability of coal. *Int. J. Rock Mech. Min.* **1975**, *12*, 129−145.
(94) Bredehoeft, J. D.; Wolf, R. G.; Keys, W. S.; Shutter, E. Hydraulic fracturing to determine the regional in situ stress field in the Piceance Basin, Colorado. *Geol. Soc. Am. Bull.* **1976**, *87*, 250−258.
(95) Haimson, B.; Fairhurst, C. In-situ Stress Determination at Great Depth by Means of Hydraulic Fracturing. In *Rock Mechanics—Theory and Practice*, Somerton, W. H., Ed.; AIME: New York, USA, pp. 1970; 559−584.
(96) Haimson, B. C.; Cornet, F. H. ISRM suggested methods for rock stress estimation-part 3: hydraulic fracturing (HF) and/or hydraulic testing of pre-existing fractures (HTPF). *Int. J. Rock Mech. Min.* **2003**, *40*, 1011−1020.
(97) Hou, Q.; Li, H.; Fan, J.; Ju, Y.; Wang, T.; Li, X.; Wu, Y. Structure and coalbed methane occurrence in tectonically deformed coals. *Sci. China Earth Sci.* **2012**, *55*, 1755−1763.
(98) GB/T 30050−2013, 2013. *Classification of Coal-body Structure* (in Chinese).
(99) Wang, H.; Yan, D. *Brief Tutorial of Coal Geology*, 1st ed.; China University of Geosciences Press: Wuhan, China, 2015; pp. 131−134.

https://doi.org/10.1021/acsomega.2c00371
ACS Omega 2022, 7, 17063−17074